BEVA2.0: Modular Assembly of Golden Gate-Compatible Vectors with Expanded Utility for Genetic Engineering

Barney A. Geddes[a]*, Riley Williamson[a], Jake Schumacher[a], Ahmad Ardi[a], Garrett Levin[a], Emily Červenka[b], Rui Huang[b] and George C. diCenzo[b]

[a] Department of Microbiological Sciences, North Dakota State University, Fargo, ND, USA.
[b] Department of Biology, Queen's University, Kingston, ON, Canada.

* Corresponding Author: Barney Geddes, barney.geddes@ndsu.edu

Abstract

This expansion for the modular vector assembly platform BEVA (Bacterial Expression Vector Archive) introduces 11 new BEVA parts including two new cloning site variants, two new antibiotic resistance modules, three new origins of replication, and four new accessary modules. As a result, the modular system is now doubled in size and expanded in its capacity to produce diverse replicating plasmids. Furthermore, it is now amenable to genetic engineering methods involving genome-manipulation of target strains through deletions or integrations. In addition to introducing the new modules, we provide several BEVA-derived Golden Gate cloning plasmids that are used to validate parts and that may be useful for genetic engineering of proteobacteria and other bacteria. We also introduce new parts to allow compatibility with the CIDAR MoClo parts libraries.

Keywords

Synthetic biology, Golden Gate cloning, Genetic engineering, Plasmid

Introduction

Since its inception, Golden Gate DNA assembly technology has revolutionized the ability to rapidly assemble multiple fragments of DNA in linear orders, facilitating advancements in synthetic biology (Engler *et al.*, 2009). This technique, particularly through the MoClo (Modular Cloning) system, has enabled the hierarchical assembly of genetic constructs using standardized parts, making it a powerful tool for researchers. MoClo's early adoption was largely driven by plant science research, where it was used to develop constructs for plant engineering via *Agrobacterium* tDNA integration (Werner *et al.*, 2012). This led to the creation of extensive parts libraries and kits for plant engineering, such as those available through Addgene, which include promoters, untranslated regions, antigen tags, subcellular localization signals, marker genes, and terminators (Weber *et al.*, 2011; Werner *et al.*, 2012; Engler *et al.*, 2014; Gantner *et al.*, 2018), as well as tools for genome editing (Hahn *et al.*, 2020; Grützner *et al.*, 2021; Stuttmann *et al.*, 2021). These resources have significantly accelerated synthetic biology by allowing researchers to rapidly assemble complex constructs using standardized parts.

While initially focused on plant engineering, the MoClo system naturally expanded to other organisms, including microorganisms. For example, parts kits have been developed for yeast hierarchical assembly (Lee *et al.*, 2015) and protein expression (Obst, Lu and Sieber, 2017), and the CIDAR MoClo Library was developed for bacteria (Iverson *et al.*, 2016), which includes a variety of useful synthetic biology parts sourced from the iGEM Registry of Standard Biological Parts. A CIDAR MoClo Expansion was also released that includes even more promoters, ribosome binding sites, coding sequences, and terminators, further enhancing its utility in synthetic biology. Useful systems for protein expression in *Escherichia coli* have also been developed (Moore *et al.*, 2016; Bentham *et al.*, 2021). However, with the widespread adoption of Golden Gate cloning, and new parts libraries in research labs around the world, there has been a growing need for new Golden Gate-compatible vectors with utility in a wide variety of organisms. To address this, we previously developed the Bacterial Expression Vector Archive (BEVA), a system that enables the assembly of Golden Gate cloning vectors from a library of standardized parts using a MoClo-like hierarchical assembly approach (Geddes, Mendoza-Suárez and Poole, 2019).

The field of microbial engineering continually seeks more efficient and versatile methods for designing plasmids to deliver and express genetic cargo. BEVA and the Standard European

Vector Architecture (SEVA) (Silva-Rocha *et al.*, 2013), which was recently adapted for Golden Gate cloning (Martínez-García *et al.*, 2023), have emerged as promising tools due to their modular approach and ease of vector design, offering a path toward high-throughput applications. These models streamline the process of assembling complex genetic constructs by providing standardized, interchangeable modules that can be easily arranged in various configurations.

In this work, we report the creation of 11 new modules that significantly expand the utility of BEVA. We also generate and validate the performance of several new Golden Gate vectors that utilize the modules. The new vectors expand the utility of BEVA in two ways. First, they increase the capacity to generate useful expression vectors for diverse bacterial taxa by incorporating additional antibiotic resistance genes and broad host range origins of replication. Second, they incorporate modules that allow the generation of vectors useful for bacterial genome engineering, either through homologous or site-specific recombination. Overall, this study not only expands the BEVA toolkit but also contributes to the broader goal of developing versatile and efficient plasmid systems for microbial engineering.

Materials and Methods

Design of new BEVA modules

New BEVA modules were designed based on functional units from pre-existing cloning vectors and synthesized free of internal BsaI, BpiI (BbsI) and BsmBI (Esp3I) sites by Twist Bioscience in the Amp^R backbone "pTwist Amp High Copy", Cm^R backbone "pTwist Chlor High Copy, or cloned via BsaI into Cm^R pGGAselect (New England Biolabs). In some cases, prototypes were designed by PCR amplification and cloning into pJet1.2, with the resulting vectors then used for generating Level 1 cloning vectors (pQGG002-005). However, these modules were later recloned into pGGAselect or resynthesized in the pTwist Chlor/Amp High Copy plasmids to eliminate a BsaI site from the pJet1.2 backbone that caused cloning efficiency issues.

Golden Gate cloning sites

Two new Level 1 cloning site modules were generated by altering the Level 1 cloning site from pOGG004. For pNDGG021 and pNDGG022, we excluded the T0 terminator 3' of the cloning site. For pNDGG022, we further altered the 5' BsmB1(Esp31) fusion site to CAGA to allow by-

passing of the endlinker/terminator modules that include the *rrnB* T1 terminator and to allow for directly connecting these modules to a Position 4 module 3' fusion site, thus completely excluding terminators flanking Level 1 cloning sites.

Antibiotic resistance cassettes

Antibiotic resistance modules were flanked by 5' BsmB1(Esp31)-GCAA and 3' ACTA-BsmB1(Esp31) sites to enable cloning as Position 2 modules in BEVA. For the kanamycin/neomycin resistance gene *nptII* (in pNDGG001), we used 1,036 bp from the cloning vector pTH1937 (Milunovic *et al.*, 2014) that included the *nptII* open reading frame and 241 bp upstream which was cloned into pGGAselect via BsaI. For the spectinomycin resistance gene *aadA* (in pNDGG002), we synthesized 1,786 bp from the pHP45Ωspec interposon (Prentki and Krisch, 1984) that contained the *aadA* open reading frame with 516 upstream and 259 bp downstream regions in pTwist Amp High Copy.

Origins of replication and transfer

Three new origins of replication and transfer were generated. These modules were each flanked by 5' BsmB1(Esp31)-ACTA and 3' TTAC-BsmB1(Esp31) sites to enable cloning as Position 3 modules in BEVA. The sequences of the origins p15A (pNDGG006) and pMB1 (pNDGG007), including their *oriT*s, were derived from 1,492 bp and 980 bp segments from pTH1937 (Milunovic *et al.*, 2014) and pUCP30T (Schweizer, Klassen and Hoang, 1996), respectively. pMB1 was cloned into pGGAselect via BsaI, while p15A was synthesized in pTwist Chlor High Copy. The broad host range origin RSF1010 (3,078 bp) was PCR amplified from pRSF-LtetO-GFP (Lee *et al.*, 2019) and combined with a 268 bp *oriT* amplified from pOGG026 (Geddes, Mendoza-Suárez and Poole, 2019) by BsaI Golden Gate cloning into pGGAselect to generate pNDGG005.

Accessory modules

Four accessory modules were added, each flanked with 5' BsmB1(Esp31)-TTAC and 3' CAGA-BsmB1(Esp31) sites to enable cloning as Position 4 modules in BEVA. The *sacB* gene enabling sucrose counterselection was designed based off of pJQ200SK (Quandt and Hynes, 1993), and

the resulting module in pNDGG008 included 1,944 bp surrounding the *sacB* open reading frame including 446 bp upstream and 76 bp downstream.

The *FRT* site-specific Flp recombinase motif (GAAGTTCCTATTCCGAAGTTCCTATTCTCTAGAAAGTATAGGAACTTC) was synthesized as a Position 4 module in pNDGG009 with a few extra flanking base pairs to bring the total size to 63 bp. The *attP* ϕC31 integrase target site (CCCCAACTGGGGTAACCTTTGAGTTCTCTCAGTTGGGGG) was similarly synthesized as a Position 4 module in pNDGG010. An *attP* motif was also included in pNDGG009 flanked by BsaI (5'GCTT and 3'CGCT) sites (CIDAR EF module) such that it could be added to the 3' end of an open reading frame in a Level 1 cloning. Likewise, a *FRT* motif flanked by the same BsaI sites (5'GCTT/3'CGCT) was added to pNDGG010.

The I-SceI site accessary module in pQGG001 was generated by ligating the I-SceI site as an annealed double-stranded oligomer (5' – TCTGGACTACGGTTCCAAATTACCCTGTTATCCCTACCTTGGAATGGTCA - 3' and 5'- TTACTGACCATTCCAAGGTAGGGATAACAGGGTAATTTGGAACCGTAGTC - 3') into an *Esp3I*-digested pOGG012 backbone using T4 DNA ligase.

CIDAR terminators

Three terminators from CIDAR (T2m, T12m and T15m from CIDAR MoClo Extension Volume I) were adapted such that the 3' fusion site matched BEVA L1 cloning vectors. The fusion site was adapted during cloning as a Level 0 part into pOGG006. The same forward primer was used for all three, which bound upstream of the 5' BsaI site and added a BpiI fusion site (TGCC) for cloning into pOGG006 (5'- AAAGAAGACAATGCCCGGCCGCTTCTAGAGA-3'). A unique 3' primer was used for each, with the binding site anchored in the terminator and an altered 3' BsaI fusion site added in the primer along with a BpiI fusion site for cloning into pOGG006 (T2m = 5'-AAAGAAGACAATCCCGGTCTCAAGCGTCTCAAGGGCGCAATAAAA-3'; T12m = 5'-AAAGAAGACAATCCCGGTCTCAAGCGTTGAGAAGAGAAAAGAAAACCG-3', T15m = 5'-AAAGAAGACAATCCCGGTCTCAAGCGGGCAGACCAGAAACAAA-3'. After cloning into pOGG006, the resulting plasmids functioned as Level 0 parts, for BEVA, flanked by *BsaI* and the fusion sites GCTT (5') and CGCT (3').

Golden Gate cloning

Golden Gate cloning reactions were performed using forty fmol of plasmid parts in a reaction mix recipe of 1 µl restriction enzyme (BsmBI-v2, Esp3I, or BsaI-HF-v2) (New England Biolabs), 1.5 µl bovine serum albumin, 1 µl T4 DNA ligase (400 units/µL; New England Biolabs), and 1.5 µl 10x T4 DNA ligase buffer, diluted with ddH_2O to a total volume of 15 µl. Alternatively, NEB Golden Gate Assembly Kits (BsaI-HF-v2 or BsmBI-v2) were used as a pre-mixed reaction mix with the DNA parts and ddH_2O. The Golden Gate cloning reactions were performed in a thermocycler as follows: For BbsI/Esp3I: 30 cycles of 42°C for 1 minute followed by 16°C for 1 minute, with heat inactivation at 60°C for 5 minutes; for BsaI: 30 cycles of 37°C for 1 minutes and 16°C for 1 minute, with heat inactivation at 60°C for 5 minutes. The resulting reaction mixes were stored at -20ºC before thawing and using to transform chemically competent *E. coli* DH5α. Successful transformants were selected using appropriate antibiotics and X-gal (5-bromo-4-chloro-3-indolyl-β-D-galactopyranoside). Successful vector constructions were selected based on blue-colored colonies, while successful Level 1 clonings were selected based on white-colored colonies. Plasmids were verified by diagnostic restriction digest and/or whole plasmid long-read sequencing by Plasmidsaurus.

Genetic manipulations

Bacterial strains used in this work are listed in **Table 1**. *E. coli* and *Sinorhizobium meliloti* strains were grown in liquid or solid Lysogeny Broth (LB) medium, supplemented with 0.25 mM $MgCl2_2$ and 0.25 mM $CaCl_2$ (termed LBmc) for *S. meliloti. E. coli* strains were grown at 37°C while *S. meliloti* strains were grown at 28°C. Antibiotics were added to media when necessary for *E coli* (Ec) or *S. meliloti* (Sm), at the following concentrations: gentamicin 10 µg/ml (Ec) or 60 µg/ml (Sm), kanamycin 25 µg/ml (Ec), neomycin 200 µg/ml (Sm), spectinomycin 50 µg/ml (Ec) or 100 µg/ml (Sm), ampicillin 100 µg/ml (Ec), and tetracycline 5 µg/ml (Ec or Sm). Sucrose counterselection was performed by adding 10% sucrose to LB medium. Conjugations between *E. coli* and *S. meliloti* were performed by triparental mating using *E. coli* MT616 as a helper strain (Finan *et al.*, 1986). Tests for colony antibiotic resistance/sensitivity phenotypes were performed by patching colonies onto replicated agar plates using a sterilized toothpick. Transformation into *E. coli* and conjugation into *S. meliloti* by triparental mating were performed using routine protocols (Finan *et al.*, 1986; Geddes, Mendoza-Suárez and Poole, 2019).

Fluorescence measurements by flow cytometry and plate reader assays

Preparation of cells for flow cytometry experiments were conducted as follows. Cells were grown in LB media containing standard working concentrations of the antibiotic corresponding to the plasmid-encoded resistance. Media was inoculated with a single colony and placed on a shake incubator set to 37°C at 215 rpm and grown overnight. One ml of each cell culture was transferred to individual 1.5 ml microtubes, after which their optical density was measured using a spectrophotometer. The tubes were then centrifuged for one minute at 17,000 x g. The supernatant was removed, and the pellet was resuspended in PBS (phosphate-buffered saline) to a final OD600 (optical density at 600 nm) of 1.0. Resuspended cells were further diluted 1:100 in PBS immediately prior to flow cytometry. Tubes containing the diluted samples were placed in the flow cytometer receptacle one at a time. The Beckman Cytoflex S flow cytometer was set to interrogate the cells using yellow and blue lights. The yellow light detectors were set to measure an mScarlet-I band path of 585/42, and the blue light detectors were set to measure both GFP at 525/40 and SSC at 488/8. Speed settings were adjusted to reach an average of 1000 events per second. These settings were adjusted depending on each sample but were generally kept at the lowest speed of 10 µl/min. Samples were manually compensated when required.

For measurements of fluorescence by plate reader, a Cytation 5 was used to quantify fluorescence across a bacterial growth curve. *E. coli* or *S. meliloti* were grown at 37ºC and 28ºC, respectively, for 24 hours from a starting OD600 of 0.05. The OD600 and fluorescence was measured every 20 minutes. The growth was analyzed using the Growthcurver package in R. The fluorescent values presented are derived from the maximum doubling time in the growth curve. The following parameters were used for fluorescent measurements: cfCFP - excitation 485, emission 475, gain 90; sfGFP - excitation 485, emission 510, gain 60; sfYFP - excitation 510, emission 535, gain 100; mScarlet-I - excitation 569, emission 593, gain 108.

Results and Discussion

Expansion of BEVA with 11 new modules.

We aimed to improve the utility of BEVA for the construction of useful Golden Gate vectors by (1) expanding the potential host range with additional broad host range origin of replication and antibiotic resistance modules, and (2) expand the utility to routinely used vectors for genome

manipulations (deletions/integrations) via the addition of narrow host range origins of replication, counters-electable markers, and site-specific recombinase sites. To enable this, we designed 11 new modules that are shown as part of the broader BEVA archive in **Figure 1** and listed in **Table 1**. The rational for inclusion of each of the modules is described below.

The initial BEVA was largely designed as a platform for generating expression vectors and hence included the broad host range origins of replication pBBR1 (Antoine and Locht, 1992) and RK2 (Meyer, Figurski and Helinski, 1975) with several options for antibiotic resistance genes that could be tailored to a target strain of interest. To facilitate wider host utility, we added another widely-used broad host range origin of replication, RSF1010 (Guerry, Van Embden and Falkow, 1974; Scholz *et al.*, 1989), as a Position 3 module (vector pNDGG005). We also expanded available antibiotic selection by adding spectinomycin resistance via an *aadA* cassette (Prentki and Krisch, 1984) as a Position 2 module (vector pNDGG002). While a kanamycin/neomycin resistance module (*aphA*-based) was available in the original BEVA, we and others have found this module to be ineffective for neomycin-based selection in *Sinorhizobium meliloti* (personal communication). Therefore, a new kanamycin/neomycin module was added based on the more widely used *nptII* gene (Yenofsky, Fine and Pellow, 1990) (vector pNDGG001).

Genome manipulations in model bacteria such as *S. meliloti* 1021 routinely involve the use of integrative, or "suicide", plasmids that replicate readily in *E. coli* but must integrate into the genome to be maintained in the target microbe (Prentki and Krisch, 1984). Integrations can be catalyzed by cloning a short sequence of the target genome to facilitate integration at a specific genomic locus via homologous recombination. Double homologous recombination can generate deletions in a similar approach by including target-genome sites flanking a region to be deleted and incorporating a counter-selectable marker in the vector backbone to catalyze its excision. An alternative to homologous recombination is to utilize site-specific recombinases to catalyze integration at a target site in the host genome with a compatible recombinase target sequence of an integrative plasmid (diCenzo and Finan, 2018). These approaches can also be combined to catalyze inversions or large deletions between two recombinase sites, following their integration on either side of a target region via two heterologous integrative vector backbones. To facilitate all of these approaches, we added two narrow host range origins (p15A (Chang and Cohen, 1978) and pMB1 (Rossi *et al.*, 1996), vectors pNDGG006-7), two site-

specific recombinase sites (*FRT* (Cox, 1983) and *attP* (Kuhstoss and Rao, 1991; Thorpe and Smith, 1998), vectors pNDGG009-10), and two counter-selectable markers (I-SceI and *sacB*, vectors pQGG001 and pNDGG008, respectively). The I-SceI target sequence can be counter-selected through expression of the I-SceI restriction enzyme from an introduced plasmid (Aubert, Hamad and Valvano, 2014), while *sacB* can be counter-selected via sucrose toxicity (Quandt and Hynes, 1993). The *FRT* and *attP* sites facilitate recombination with *FRT* and *attP* sites via Flp recombinase and ϕC31 integrase, respectively (diCenzo and Finan, 2018). The availability of two heterologous narrow host range origins facilitates introductions of multiple plasmids by homologous recombination (such as for *FRT*-mediated deletions), minimizing the chance for recombination between them (diCenzo and Finan, 2018). To allow further minimization of homology between assembled plasmids, we also introduced two alternate Level 1 cloning sites (pNDGG021-22) that allow exclusion of the 3' T0 terminator or the 5' T1 terminator (via skipping an endlinker) from assembled vectors.

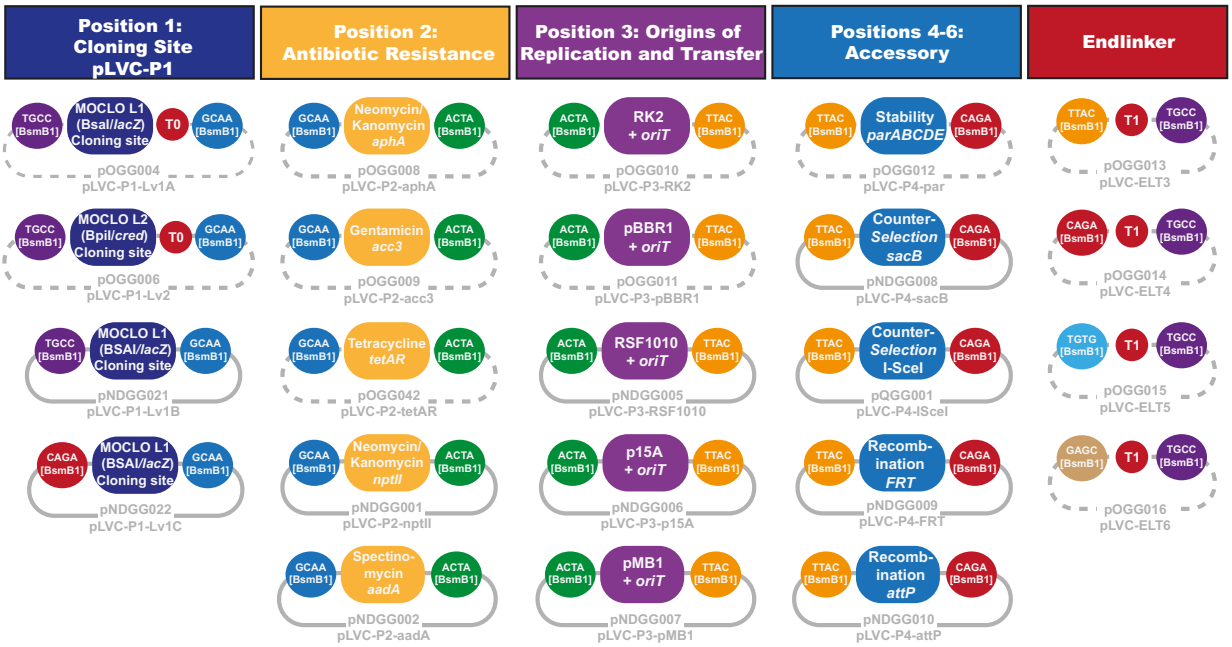

Figure 1. Diagram of vector modules in the expanded BEVA2.0 vector archive. Dashed vector backbones reflect modules from BEVA1.0 (Geddes, Mendoza-Suárez and Poole, 2019). Solid vector backbones reflect BEVA2.0 expansion modules presented in this work. Colored rounded rectangles reflect parts, colored by module type. Colored circles reflect sticky overhangs

generated by *BsmB1* and ligated by DNA ligase in Golden Gate cloning reactions. Plasmid names are indicated on the backbone with appropriate BEVA nomenclature below.

A suite of broad host range Golden Gate expression vectors

Using the updated BEVA2.0 parts library, we combined several modules with the aim of developing a flexible broad host range vector suite with varied antibiotic resistance. To this end, we included four antibiotic resistance modules (*aadA* (Sp), *nptII* (Nm/Km), *tetAR* (Tc), and *acc3* (Gm); Position 2) with three broad host range origins of replication (RK2, pBBR1 and RSF1010; Position 3). These were combined in the standard BEVA architecture with a Level 1 Golden Gate cloning site (Position 1), the *par* accessary cluster for stability in the absence of antibiotic selection (Position 4), and an endlinker (ELT4). The resulting vectors, their compositions and are summarized in **Table 1** and **Figure 2A** with appropriate BEVA nomenclature (Geddes, Mendoza-Suárez and Poole, 2019)**.**

While the *parABCDE* cluster has been characterized for its ability to stabilize RK2 plasmids from which it was derived, we wished to verify the compatibility of this module with the heterologous origins of replication pBBR1 and RSF1010. To do so, we performed an experiment to assess plasmid stability in the absence of antibiotic selection, and compared the stability of plasmids that included the module (Lv1-Gm-pBBR1-par-ELT4, and Lv1-Gm-RSF1010-par-ELT4) to vectors we constructed the excluded the *par* module (Lv1-Gm-pBBR1-ELT3, and Lv1-Gm-RSF1010-ELT3). Single colonies of *E. coli* transformants from each plasmid were used to inoculate an overnight culture in the absence of antibiotics. Following overnight growth and saturation, the culture was plated by serial dilution to single colonies without antibiotic selection, and one hundred resulting colonies were patched onto Gm to assess plasmid maintenance. In this experiment, while the pBBR1 vector showed stability in either the presence or absence of *par*, the RSF1010 plasmid was significantly more stable when including the *par* module (**Figure 2B**).

To verify Level 1 cloning and suitability of plasmids for expression, one plasmid from each origin of replication from the suite (all Tc^R) were used for Level 1 Golden Gate cloning, wherein we combined sfGFP with a constitutive promoter and ribosome binding site in *E. coli* ST18ALA (**Table 1**). The fluorescence of the resulting plasmids was tested using flow cytometry

and we found significant levels of GFP fluorescence in plasmids that contained RK2, pBBR1, or RSF1010 backbones. While RK2 and pBBR1 plasmids showed similar profiles that were clearly distinct from non-fluorescent control cells, the RSF1010 backbone yielded a significant subpopulation of non-fluorescent cells (**Figure 2C**).

Table 1. Plasmids used in this work

Vector Name	BEVA Nomenclature	Description	Citation
Vector construction parts used to assemble BEVA2.0 vectors (pLVC)			
Position 1: cloning sites (pLVC-P1)			
pOGG004	pLVC-P1-Lv1A	BEVA Position 1 Level 1 BsaI cloning site flanked by T0, Sp^R. Addgene 113979	(Geddes, Mendoza-Suárez and Poole, 2019)
pOGG006	pLVC-P1-Lv2	BEVA Position 1 Level 2 BpiI cloning site flanked by T0, Sp^R. Addgene 113981	(Geddes, Mendoza-Suárez and Poole, 2019)
pNDGG021	pLVC-P1-Lv1B	BEVA2.0 Position 1 Level 1 BsaI cloning site without T0, Amp^R	This work
pNDGG022	pLVC-P1-Lv1C	BEVA2.0 Position 1 Level 1 BsaI cloning site with alternate CAGA 3' fusion site, without T0, Amp^R	This work
Position 2: antibiotic resistance cassettes (pLVC-P2)			
pOGG008	pLVC-P2-aphA	BEVA Position 2 Km/Nm antibiotic resistance via *aphA*, $Sp^R/Km^R/Nm^R$. Addgene 113982	(Geddes, Mendoza-Suárez and Poole, 2019)
pOGG009	pLVC-P2-acc3	BEVA Position 2 Gm antibiotic resistance via *aac3*, Sp^R/Gm^R. Addgene 113983	(Geddes, Mendoza-Suárez and Poole, 2019)
pOGG042	pLVC-P2-tetAR	BEVA Position 2 Gm antibiotic resistance via *aac3*, Sp^R/Gm^R. Addgene 113998	(Geddes, Mendoza-Suárez and Poole, 2019)
pNDGG001	pLVC-P2-nptII	BEVA2.0 Position 2 Km/Nm antibiotic resistance via *nptII*, $Cm^R/Km^R/Nm^R$.	This work
pNDGG002	pLVC-P2-aadA	BEVA2.0 Position 2 Sp antibiotic resistance via *aadA*, Amp^R/Sp^R	This work
Position 3: origins of replication and transfer (pLVC-P3)			
pOGG010	pLVC-P3-RK2	BEVA Position 3 RK2 broad host range origin of replication with *oriT*, Sp^R. Addgene 113984	(Geddes, Mendoza-Suárez and Poole, 2019)

pOGG011	pLVC-P3-pBBR1	BEVA Position 3 pBBR1 broad host range origin of replication with *oriT*, Sp^R. Addgene 113985	(Geddes, Mendoza-Suárez and Poole, 2019)
pNDGG005	pLVC-P3-RSF1010	BEVA2.0 Position 3 RSF1010 broad host range origin of replication with *oriT*, Cm^R.	This work
pNDGG006	pLVC-P3-p15A	BEVA2.0 Position 3 p15A narrow host range origin of replication with *oriT*, Cm^R.	This work
pNDGG007	pLVC-P3-pMB1	BEVA2.0 Position 3 pMB1 narrow broad host range origin of replication with *oriT*, Cm^R.	This work
Position 4: accessary modules (pLVC-P4-6)			
pOGG012	pLVC-P4-par	BEVA Position 4 *parCDABE* stability locus, Sp^R. Addgene 113986	(Geddes, Mendoza-Suárez and Poole, 2019)
pNDGG008	pLVC-P4-sacB	BEVA2.0 Position 4 *sacB* sucrose counterselection module, Amp^R.	This work
pQGG001	pLVC-P4-ISceI	BEVA2.0 Position 4 I-SceI recognition/cut site, Sp^R.	This work
pNDGG009	pLVC-P4-FRT	BEVA2.0 Position 4 *FRT* recombinase site, Amp^R. Also includes *attP* EF module for L1 GG cloning.	This work
pNDGG010	pLVC-P4-attP	BEVA2.0 Position 4 *attP* recombinase site, Amp^R. Also includes *FRT* EF module for L1 GG cloning.	This work
Endlinkers (ELT)			
pOGG013	pLVC-ELT3	BEVA Position 3 endlinker with T1 terminator, Sp^R. Addgene 113987	(Geddes, Mendoza-Suárez and Poole, 2019)
pOGG014	pLVC-ELT4	BEVA Position 4 endlinker with T1 terminator, Sp^R. Addgene 113988	(Geddes, Mendoza-Suárez and Poole, 2019)
pOGG015	pLVC-ELT5	BEVA Position 5 endlinker with T1 terminator, Sp^R. Addgene 113989	(Geddes, Mendoza-Suárez and Poole, 2019)
pOGG016	pLVC-ELT6	BEVA Position 6 endlinker with T1 terminator, Sp^R, Addgene 113990	(Geddes, Mendoza-Suárez and Poole, 2019)
BEVA2.0 vectors used for Level 1 or 2 Golden Gate cloning			
pNDGG003	Lv1A-tetAR-RK2-par-ELT4	BEVA2.0 Broad host range plasmid with stability. Golden Gateassembly from pOGG010, pOGG012, pOGG014, pOGG042, and pOGG004, Tc^R	This work
pNDGG004	Lv1A-tetAR-pBBR1-par-ELT4	BEVA2.0 Broad host range plasmid with stability. Golden Gate assembly from pOGG011, pOGG012, pOGG014, pOGG042, and pOGG004, Tc^R	This work
pNDGG049	Lv1A-aac3-pBBR1-par-ELT4	BEVA2.0 Broad host range plasmid with stability. Golden Gate assembly from pOGG004, pOGG009, pOGG011, pOGG012, and pOGG014, Gm^R	This work
pNDGG050	Lv1A-aac3-RK2-par-ELT4	BEVA2.0 Broad host range plasmid with stability. Golden Gate assembly from pOGG004, pOGG009, pOGG010, pOGG012, and pOGG014, Gm^R	This work

pNDGG051	Lv1A-aadA-pBBR1-par-ELT4	BEVA2.0 Broad host range plasmid with stability. Golden Gate assembly from pOGG004, pNDGG002, pOGG011, pOGG012, and pOGG014, Sp^R	This work
pNDGG052	Lv1A-aadA-RK2-par-ELT4	BEVA2.0 Broad host range plasmid with stability. Golden Gate assembly from pOGG004, pNDGG002, pOGG010, pOGG012, and pOGG014, Sp^R	This work
pNDGG053	Lv1A-nptII-pBBR1-par-ELT4	BEVA2.0 Broad host range plasmid with stability. Golden Gate assembly from pOGG004, pNDGG001, pOGG011, pOGG012, and pOGG014, Nm^R/Km^R	This work
pNDGG054	Lv1A- nptII-RK2-par-ELT4	BEVA2.0 Broad host range plasmid with stability. Golden Gate assembly from pOGG004, pNDGG001, pOGG010, pOGG012, and pOGG014, Nm^R/Km^R	This work
pNDGG056	Lv1A- aac3-RSF1010-par-ELT4	BEVA2.0 Broad host range plasmid with stability. Golden Gate assembly from pOGG004, pOGG009, pNDGG005, pOGG012, and pOGG014, Gm^R	This work
pNDGG057	Lv1A-tetAR-RSF1010-par-ELT4	BEVA2.0 Broad host range plasmid with stability. Golden Gate assembly from pOGG004, pOGG042, pNDGG005, pOGG012, and pOGG014, Tc^R	This work
pNDGG058	Lv1A-aadA-RSF1010-par-ELT4	BEVA2.0 Broad host range plasmid with stability. Golden Gate assembly from pOGG004, pNDGG002, pNDGG005, pOGG012, and pOGG014, Sp^R	This work
pNDGG059	Lv1A-nptII-RSF1010-par-ELT4	BEVA2.0 Broad host range plasmid with stability. Golden Gate assembly from pOGG004, pNDGG001, pNDGG005, pOGG012, and pOGG014, Nm^R/Km^R	This work
pNDGG070	Lv1A-aadA-pBBR1-sacB-ELT4	BEVA2.0 Sucrose curable broad host range plasmid. Golden Gate assembly from pOGG004, pNDGG002, pOGG011, pNDGG008, and pOGG014, Sp^R	This work
pQGG002	Lv1A-nptII-p15A-ISceI-ELT4	BEVA2.0 Narrow host range plasmid with I-SceI counterselectable site. Golden Gate assembly from pOGG004, pNDGG001, pNDGG006, pQGG001, pOGG014. Km^R/Nm^R.	This work
pQGG003	Lv2-nptII-p15A-ISceI-ELT4	BEVA2.0 Narrow host range plasmid with I-SceI counterselectable site for BpiI cloning. Golden Gate assembly from pOGG006, pNDGG001, pNDGG006, pQGG001, pOGG014. Km^R/Nm^R.	This work
pQGG004	Lv1A-aac3-p15A-ISceI-ELT4	BEVA2.0 Narrow host range plasmid with I-SceI counterselectable site. Golden Gate assembly from pOGG004, pOGG009, pNDGG006, pQGG001, pOGG014. Gm^R.	This work
pQGG005	Lv2-aac3-p15A-ISceI-ELT4	BEVA2.0 Narrow host range plasmid with I-SceI-ELT4 counterselectable site for BpiI cloning. Golden Gate assembly from pOGG006, pOGG009, pNDGG006, pQGG001, pOGG014. Gm^R.	This work
pNDGG012	Lv1C-aac3-pMB1-FRT	Narrow host range plasmid with *FRT* site. Golden Gate assembly from pNDGG022, pNDGG007, pOGG009, pNDGG009. Gm^R.	This work
pNDGG013	Lv1C-nptII-p15A-FRT	Narrow host range plasmid with *FRT* site. Golden Gate assembly from pNDGG022, pNDGG006, pNDGG001, pNDGG009. Km^R/Nm^R.	This work
pNDGG014	Lv1B-aac3-pMB1-ELT3	Narrow host range plasmid. Golden Gate assembly from pNDGG021, pNDGG007, pOGG009, pOGG013. Gm^R.	This work
pNDGG015	Lv1B-nptII-p15A-ELT3	Narrow host range plasmid. Golden Gate assembly from pNDGG021, pNDGG006, pNDGG001, pOGG013. Km^R/Nm^R.	This work
Level 1 Golden Gate modules (pL1M)			

J23106	pL1M-AB-J23106	CIDAR Medium-strength constitutive promoter from Anderson series, AB module, Amp^R, Addgene 65992	(Iverson *et al.*, 2016)
B0032m	pL1M-BC-B0032M	CIDAR Weiss RBS of medium strength, BC module, Amp^R, Addgene 66020	(Iverson *et al.*, 2016)
BCD12	pL1M-BC-BCD12	CIDAR BiCistronic RBS of medium-low strength, BC module, Amp^R, Addgene 66023	(Iverson *et al.*, 2016)
C3m	pL1M-CD-C3m	CIDAR MoClo Extension volume I, sfGFP, CD module, Amp^R. Addgene 120956	Gift from Richard Murray via Addgene)
C51m	pL1M-CD-C51m	CIDAR MoClo Extension volume I, sfYFP, CD module, Amp^R. Addgene 120975	Gift from Richard Murray via Addgene)
C91m	pL1M-CD-C91M	CIDAR MoClo Extension volume I, sfCFP, CD module, Amp^R. Addgene 120999	Gift from Richard Murray via Addgene)
C88m	pL1M-CD-C88m	CIDAR MoClo Extension volume I, m-Scarlet-I, CD module, Amp^R. Addgene 121003	Gift from Richard Murray via Addgene)
T2m	pL1M-DE-T2m	CIDAR MoClo Extension volume I, Eck120033736 terminator (nmeth.2515), DE module, Amp^R. Addgene 121029	Gift from Richard Murray via Addgene)
T12m	pL1M-DE-T12m	CIDAR MoClo Extension volume I, Eck120026300 terminator (nmeth.2515), DE module, Amp^R. Addgene 121031	Gift from Richard Murray via Addgene)
T15m	pL1M-DE-T15m	CIDAR MoClo Extension volume I, L3S3P11 terminator (nmeth.2515), DE module, Amp^R. Addgene 121034	Gift from Richard Murray via Addgene)
pOGG037	pL1M-CE-sfGFP	BEVA1.0 sfGFP "SC" model (CE CIDAR extensions), Sp^R. Addgene 113995	(Geddes, Mendoza-Suárez and Poole, 2019)
pNDGG037	pL1M-DF-T2m	BEVA2.0 T2m terminator with DF extension for CIDAR MoClo Golden Gate Assembly, DF module. Cloned via BpiI GG Assembly of PCR amplicon into POGG006, Sp^R.	This work
pNDGG038	pL1M-DF-T12m	BEVA2.0 T12m terminator with DF extension for CIDAR MoClo Golden Gate Assembly, DF module. Cloned via BpiI GG Assembly of PCR amplicon into POGG006, Sp^R.	This work
pNDGG039	pL1M-DF-T12m	BEVA2.0 T15m terminator with DF extension for CIDAR MoClo Golden Gate Assembly, DF module. Cloned via *BpiI* GG Assembly of PCR amplicon into POGG006, Sp^R.	This work
Other plasmids			
pDA1-SceI-sacB	NA	pBBR1 broad host range plasmid expressing I-SceI homing endonuclease and *sacB* counterselectable marker, Tc^R	(Aubert, Hamad and Valvano, 2014)
pNDMS450	Lv1A-tetAR-RK2-par-ELT4 (J23106-	RK2 broad host range plasmid expressing constitutive sfGFP. GG assembly of pNDGG003_AF, J23106_AB, B0032m_BC, pOGG037_CE, and EF oligo , Tc^R	This work

	B0032m-sfGFP-oligo)		
pNDMS451	Lv1A-tetAR-pBBR1-par-ELT4 (J23106-B0032m-sfGFP-oligo)	pBBR1 broad host range plasmid expressing constitutive sfGFP. GG assembly of pNDGG004_AF, J23106_AB, B0032m_BC, pOGG037_CE, and EF oligo , Tc^R	This work
pNDMS459	Lv1A-tetAR-RSF1010-par-ELT4 (J23106-B0032m-sfGFP-oligo)	RSF1010 broad host range plasmid expressing constitutive sfGFP. GG assembly of pNDGG057_AF, J23106_AB, B0032m_BC, pOGG037_CE, and EF oligo , Tc^R	This work
pNDMS054	Lv1A-tetAR-RK2-par-ELT4 (J23106-BCD12-sfGFP-T2m)	RK2 broad host range plasmid expressing constitutive sfGFP. GG assembly from pNDGG003_AF, J23106_AB, BCD12_BC, C3m_CD, and T2m_DF (pNDGG037), Tc^R	This work
pNDMS055	Lv1A-tetAR-RK2-par-ELT4 (J23106-BCD12-sfCFP-T2m)	RK2 broad host range plasmid expressing constitutive sfCFP. GG assembly from pNDGG003_AF, J23106_AB, BCD12_BC, C91m_CD, and T2m_DF (pNDGG037), Tc^R	This work
pNDMS056	Lv1A-tetAR-RK2-par-ELT4 (J23106-BCD12-sfYFP-T2m)	RK2 broad host range plasmid expressing constitutive sfYFP. GG assembly from pNDGG003, J23106_AB, BCD12_BC, C51m_CD, and T2m_DF (pNDGG037), Tc^R	This work
pNDMS057	Lv1A-tetAR-RK2-par-ELT4 (J23106-BCD12-mScarlet-T2m)	RK2 broad host range plasmid expressing constitutive m-Scarlet-I. GG assembly from pNDGG003, J23106_AB, BCD12_BC, C99m_CD, and T2m_DF (pNDGG037), Tc^R	This work

We also demonstrated the flexibility of the BEVA system by cloning an alternate broad host range plasmid that included a module to facilitate its removal rather than promote stability, *sacB* (**Figure 2D**). We used a plasmid (Lv1-Sp-pBBR1-sacB-ELT4) to facilitate curing (i.e., loss) of the difficult to remove pBBR1 plasmids from strains of a *S. meliloti* deletion library (Milunovic *et al.*, 2014) through incompatibility. Thereafter, we found that the BEVA2.0 *sacB* plasmid was efficiently removed by sucrose counterselection (**Figure 2D**). In four replicates, *S. meliloti* bearing the Sp^R *sacB* plasmid were plated onto LBmc or LBmc with 10% sucrose by serial dilution following overnight culturing in the absence of antibiotics. Approximately 50 single colonies from each set of plates were patched onto LBmc Sp to test for plasmid loss. A low rate of plasmid loss was observed in the absence of sucrose selection, while sucrose selection resulted in a complete curing of the plasmid in the population tested.

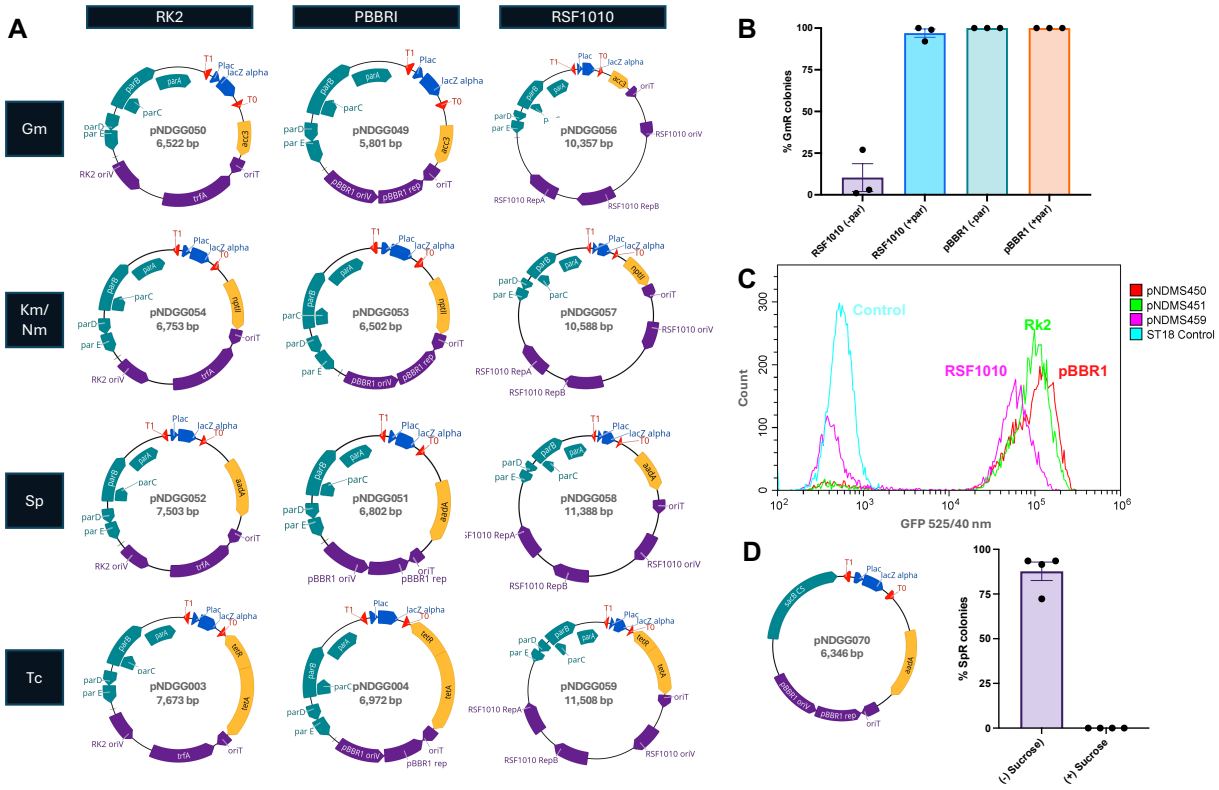

Figure 2. BEVA2.0 Broad Host Range Vectors. A. Plasmid maps of broad host range vectors developed using BEVA2.0 parts. **B.** Quantification of pBBR1 or RSF1010 plasmid maintenance with and with-out *par* loci. Data is expressed as the proportion of 100 colonies that grew on LB + Gm plates after patching following antibiotic-free culturing and spread-plating on LB. **C.** Histograms of GFP signal from flow cytometry analysis of *E. coli* ST18ALA bearing RSF1010, pBBR1, or RK2 plasmids expressing sfGFP. **D.** Plasmid map of a curable *sacB*-containing pBBR1 plasmid pNDGG070, and the proportion of plasmid loss following growth on 10% sucrose based on sensitivity when 50 colonies were patched on LB + Sp media.

Golden-Gate compatible vectors for homologous recombination

We also expanded the collection of Level 1 cloning vectors for use in genetic engineering by utilizing integrative plasmid parts from the updated BEVA2.0 parts library (Table 1). Vectors for homologous recombination were constructed using the p15A origin of replication, which generates integrative plasmids in many Gram-negative bacteria due to its inability to be maintained as a replicating plasmid (Quandt and Hynes, 1993) (Figure 3A). To facilitate

workflows for constructing deletions by double homologous recombination, we also added an I-SceI recognition site that enables curing through expression of the I-*SceI* endonuclease. We generated multiple versions including optional antibiotic selection (Gm^R or Nm^R), and two different cloning sites (BsaI or BpiI) to facilitate flexible cloning of chromosomal homologous regions, should one site or the other be present in a target region. These plasmids have been used in workflows to generate deletions in *S. meliloti* and functioned efficiently to generate marked or unmarked deletions. For example, when a pQGG004 derivative was used to create a marked deletion of the *S. meliloti phaZ* gene, the efficiency of I-SceI selection for the expected double-recombination was ~14% when averaged across four independent replicates with 17-33 colonies. Surprisingly, the efficiency varied from as low as 3% to up to 19% depending on the trial, which is a result that we have repeatedly observed when selecting for double recombinants using this approach (diCenzo, unpublished). We hypothesize that the efficiency of obtaining double recombinants varies depending on where the initial recombination occurred, and thus we recommend purifying multiple single recombinants for use in downstream steps to optimize the likelihood of obtaining a correct double recombinant.

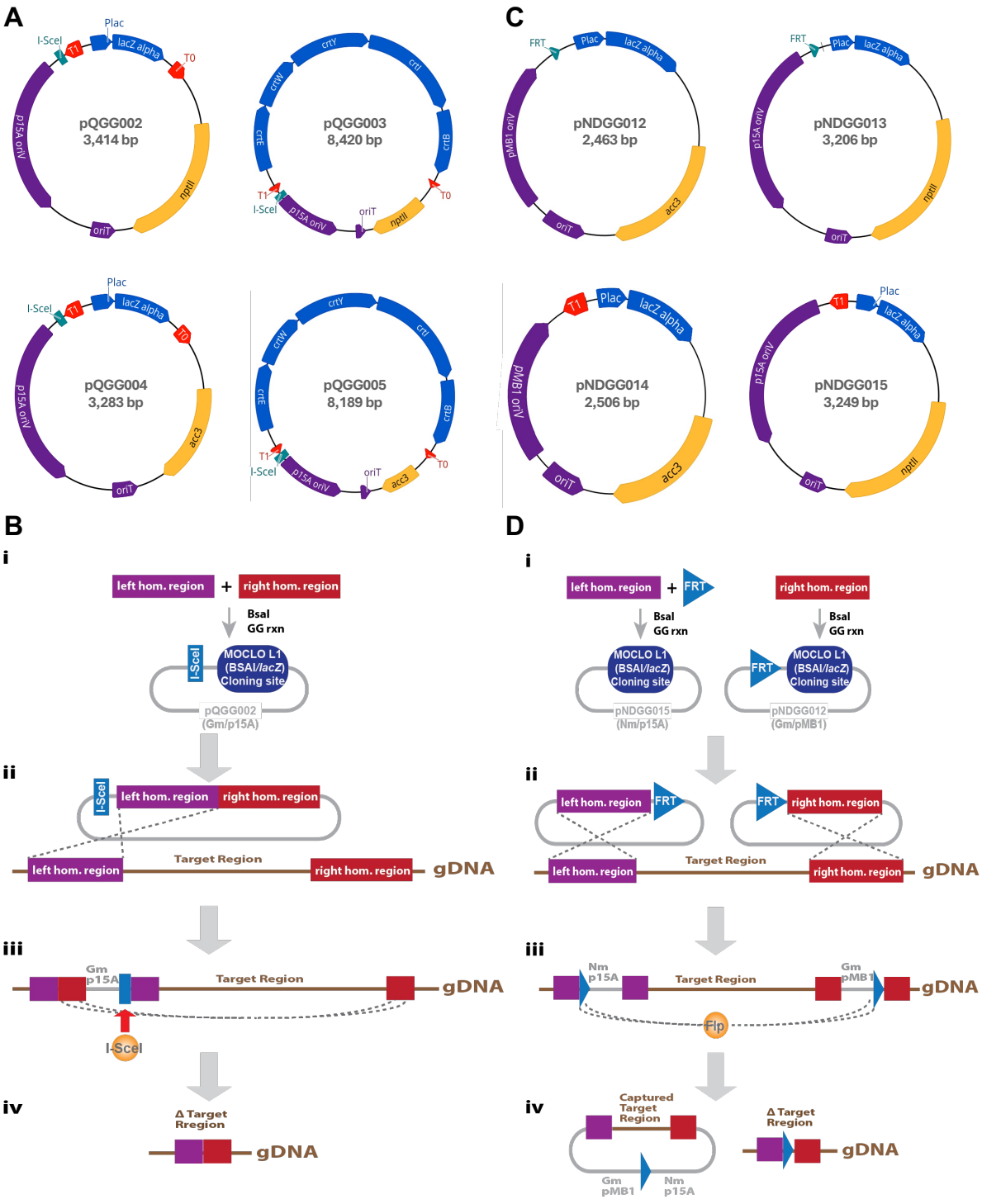

Figure 3. BEVA2.0 Genome Manipulation Plasmids. A. Maps of plasmids developed for the double homologous recombination deletion method, and **B.** schematic of the use of the plasmids to delete a target region. Steps involve: **i)** cloning of homologous regions to the left and right of

the target region into a BEVA2.0 vector using BsaI or BpiI Golden Gate cloning; **ii)** conjugating the plasmid into the target organism and selecting for integration via single cross-over homologous recombination (using antibiotic resistance on the plasmid); **iii)** introducing a replicating plasmid expressing the I-SceI endonuclease (eg. via pDA1-ISceI-sacB) by conjugation and selecting for its maintenance to select for the second recombination event, in which the BEVA2.0 plasmid backbone is excised from the genome together with the target region; and **iv)** screening resulting colonies for the presence of the deletion (based on PCR and loss of the resistance of the BEVA2.0 plasmid). **C.** Maps of plasmids developed for Flp/*FRT* recombination methods, and **D.** a schematic diagramming their use to excise and capture a target region. Steps involve: **i)** cloning homologous regions to the left and right of the target adjacent to *FRT* site in heterologous BEVA2.0 plasmids via BsaI Golden Gate cloning; **ii)** sequentially integrating the plasmids by conjugating them into the recipient and selecting for the appropriate antibiotic resistances; **iii)** introducing a replicating plasmid containing *flp* recombinase gene (eg. pTH2505) by conjugation and inducing Flp expression to catalyze excision of the target region via *FRT* recombination (optionally also introducing an *E. coli* recipient strain for region capture, and selecting with an alternate media that selects for the recipient with BEVA2.0 plasmids); and **iv)** screening for the resulting deletion by PCR and loss of BEVA2.0 backbone resistance.

Adapting the Flp/*FRT* deletion method to Golden Gate plasmid assembly

Another workflow for genetic manipulation involves the use of site-specific recombinases such as FLP, ϕC31, or Cre to generate deletions, inversions, or integrations (diCenzo and Finan, 2018). We have found these particularly useful for deleting or integrating large regions (Milunovic *et al.*, 2014; Geddes *et al.*, 2021). To adapt these workflows to Golden Gate cloning, we generated additional new integrative vectors. Since deletion workflows require sequential integration of recombinase sites flanking either side of a target, it is valuable to have a second heterologous integrative plasmid (diCenzo and Finan, 2018). It is optimal to minimize homology between the two plasmids, therefore in addition to p15A-based plasmids, we also generated integrative plasmids based on another integrative origin of replication, pMB1 and excluded the 3' T_0 terminator with an alternate Level 1 Golden Gate cloning site (Vector pNDGG0021). We used another alternate Level 1 Golden Gate cloning site (vector pNDGG0022) that both excluded the 3' T_0 terminator, and replaced the endlinker T1 terminator with an *FRT* site (vector

pNDGG009) to further expand the suite of integrative plasmids. We then designed a scheme wherein a *FRT* site can be incorporated into the 5' end of a cloned homologous region from the genome by using the *FRT*-bearing vectors, or to the 3' end of a cloned homologous region during region addition. To facilitate addition of the second *FRT* site, we generated an *FRT* site flanked by BsaI and 5' GCTT and 3' CGCT junctions (Figure 3C). We utilized these plasmids to construct an *idhA* deletion in *S. meliloti* RmP110 (Geddes, unpublished) and found them to function with similar efficiencies to traditional cloning plasmids (diCenzo and Finan, 2018).

Linking the CIDAR parts archive to BEVA plasmids.

The recently introduced CIDAR MoClo parts kit and CIDAR MoClo Expansion Volume I libraries (available as Kit 1000000059 and Kit 1000000161 through Addgene) include a wide variety of useful parts for bacterial engineering domesticated as defined parts for Level 1 Golden Gate cloning. Because both systems (CIDAR and BEVA) adopt MoClo (Weber *et al.*, 2011), both systems adopt the same fusion sites for Level 1 cloning and, as such, the systems are generally compatible. However, individual CIDAR Level 0 parts were developed with an alternate Positional architecture than BEVA or MoClo (Weber *et al.*, 2011; Iverson *et al.*, 2016; Geddes, Mendoza-Suárez and Poole, 2019) (**Figure 4A-C**). In particular, while the 5' fusion site GGAG ("A" in CIDAR) is conserved between the two systems and links to the 5' fusion site of promoter parts, the 3' cloning fusion site in BEVA is CGCT ("F" in CIDAR), whereas CIDAR was designed with terminators bearing a 3' fusion site of GCTT ("E"). Therefore, to adapt BEVA to the CIDAR architecture, we recloned several CIDAR terminators to match the 3' fusion site of BEVA plasmids (as "DF" rather than "DE" parts). Using these terminators enables researchers to utilize the wide variety of CIDAR parts for construction of open reading frames in BEVA plasmids. For example, we have cloned a variety of constitutively expressed fluorescent proteins by combining promoters, RBS, and open reading frames from CIDAR into the replicating plasmid pNDGG003 and verified their function in *S. meliloti* (**Figure 4E-H**, **Table 1**). To reflect the integration of CIDAR with BEVA we have updated BEVA Level 1 part nomenclature with the CIDAR nomenclature (**Figure 4A**, **B** and **D**, **Table 1**).

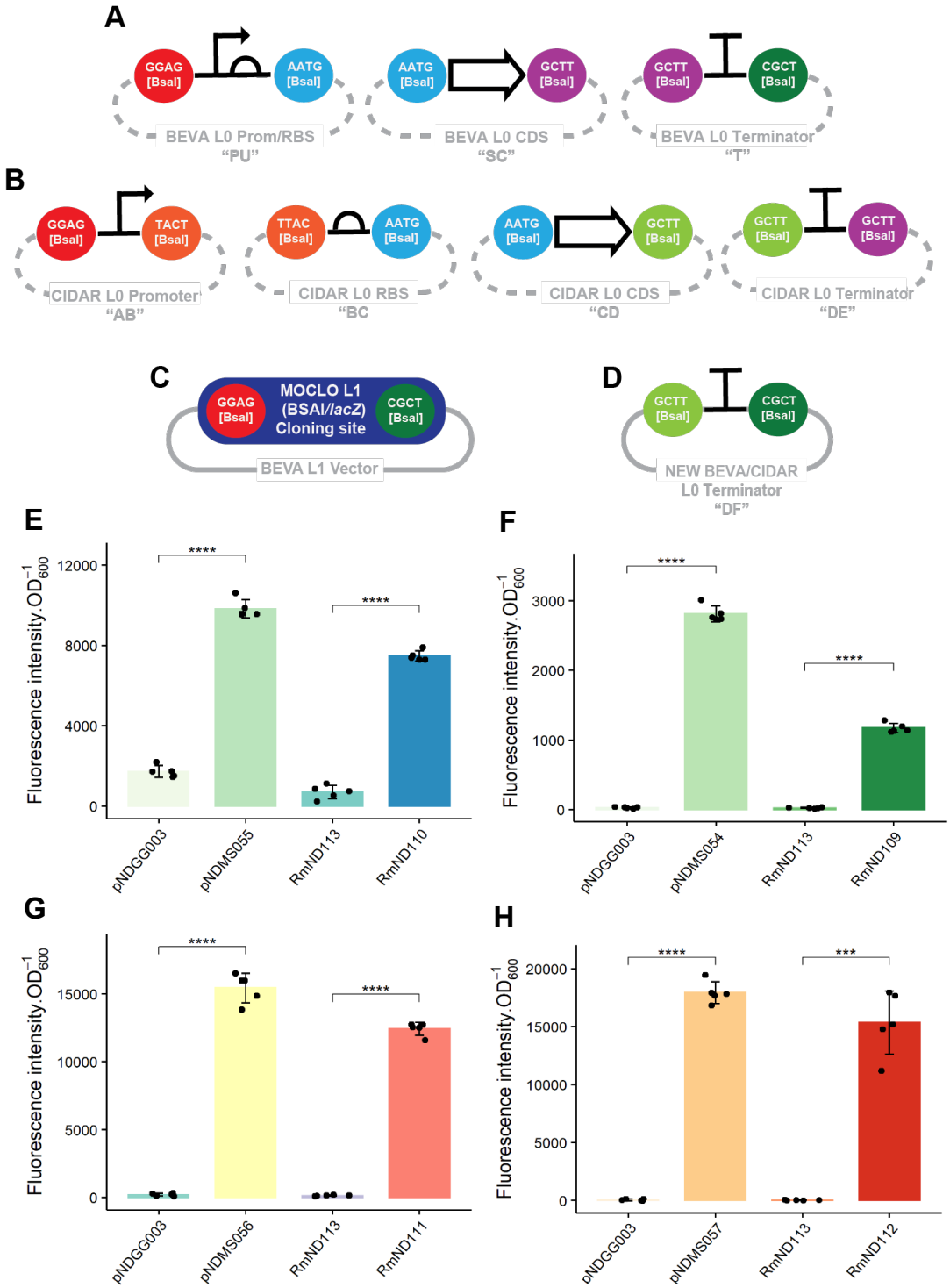

408

409 **Figure 4. Parts to link BEVA and CIDAR. A.** Diagram of the architecture of BEVA Level 0

410 parts for open reading frame construction (Geddes, Mendoza-Suárez and Poole, 2019). **B.**

411 Diagram of the architecture of CIDAR parts for open reading frame construction.

C. Architecture of a the BsaI multiple cloning site in Level 1 BEVA vectors. **D.** Architecture of BEVA/SEVA "linker" DF terminators. **E.** Fluorescence of BEVA vectors with CIDAR parts. The constitutive promoter J23106 together with the medium-strength RBS BCS12, are used to drive sfCFP (E), sfGFP (F), sfYFP (G) and mScarlet-I (H). The new linker terminator was used to assemble these marker genes in the RK2 BEVA2.0 plasmid pNDGG003. Fluorescence of the cloned plasmids in *E. coli* (pNDMS054-57) is shown next to the empty vector control (pNDGG003) on the left side of the graphs. On the right side of the graphs, *S. meliloti* RmP110 containing pNDGG003 (RmND113) is shown compared to RmP110 containing pNDMS054-57 (RmND109-112).

Conclusions

The original Bacterial Expression Vector Archive has facilitated new synthetic biology approaches for alpha-proteobacteria such as advanced strain barcoding (Mendoza-Suárez *et al.*, 2020) and adaption of CRISPR base editing (Wang *et al.*, 2021), and has supported a range of studies by streamlining genetic engineering (Geddes *et al.*, 2019; Haskett *et al.*, 2022, 2023). In addition, adaptations of the BEVA architecture have recently been performed for the development of a suite of plasmids for Tn*7* (Jorrin *et al.*, 2024) and mariner transposition (Williamson et al. in Preparation). The resources presented here in the BEVA2.0 expansion will further expand the utility of the system by extending the host range of replicating plasmids with new origins of replication and antibiotic resistance modules, introducing resources for genetic engineering by homologous or site-specific recombination, and adapting BEVA plasmids to function with the CIDAR system. We have found these upgrades to streamline genetic manipulation and mutant construction in *S. meliloti*, which is a model organism for studying symbiotic nitrogen fixation, carbon metabolism, genome evolution and sociomicrobiology (Kearsley, Sather and Finan, 2024). Moreover, the nature of the plasmid parts used indicates they should function broadly in bacteria, and have enabled approaches that probe the engineerability of diverse microbes from across the phylogenetic tree (Williamson et al. in Preparation). Overall, BEVA and BEVA2.0 represent a significant community resource for bacterial genetics and synthetic biology.

Acknowledgements

We thank Megan Ramsett and the Thomas Glass Innovation Core staff (Scott Hoselton and Kaycie Schmidt) in the Department of Microbiological Sciences, North Dakota State University for administrative and technical contributions to this work. BEVA plasmids with the pOGG prefix were a gift from Philip Poole (received from Addgene). CIDAR plasmids were a gift from Douglas Densmore (received from Addgene).

Funding

This work was supported by a New Innovator in Food & Agricultural Research (FFAR) grant to B. A. Geddes ID: FF-NIA21-0000000061m, an NSF Collaborative Research-PGR grant to B. A. Geddes: Award number 2243818. Research in the G.C.D. laboratory is supported by the Natural Sciences and Engineering Research Council of Canada (NSERC) through the Discovery Grants program (grant number RGPIN-2020-07000).

Data Availability

Golden Gate cloning plasmids generated in this work and their DNA sequence information have been submitted to Addgene (Deposit 85226, IDs 231305-2131339). Data supporting figures in the manuscript is available upon request.

Competing Interests

Barney A. Geddes is a co-founder of Lilac Agriculture Inc.

References

Antoine, R. and Locht, C. (1992) 'Isolation and molecular characterization of a novel broad-host-range plasmid from *Bordetella bronchiseptica* with sequence similarities to plasmids from Gram-positive organisms', *Molecular Microbiology*, 6(13), pp. 1785–1799. Available at: https://doi.org/10.1111/j.1365-2958.1992.tb01351.x.

Aubert, D.F., Hamad, M.A. and Valvano, M.A. (2014) 'A markerless deletion method for genetic manipulation of *Burkholderia cenocepacia* and other multidrug-resistant gram-negative bacteria', *Methods in Molecular Biology (Clifton, N.J.)*, 1197, pp. 311–327. Available at: https://doi.org/10.1007/978-1-4939-1261-2_18.

Bentham, A.R. *et al.* (2021) 'pOPIN-GG: A resource for modular assembly in protein expression vectors'. bioRxiv, p. 2021.08.10.455798. Available at: https://doi.org/10.1101/2021.08.10.455798.

Chang, A.C. and Cohen, S.N. (1978) 'Construction and characterization of amplifiable multicopy DNA cloning vehicles derived from the P15A cryptic miniplasmid', *Journal of bacteriology*, 134(3), pp. 1141–1156.

Cox, M.M. (1983) 'The FLP protein of the yeast 2-microns plasmid: expression of a eukaryotic genetic recombination system in Escherichia coli.', *Proceedings of the National Academy of Sciences*, 80(14), pp. 4223–4227.

diCenzo, G.C. *et al.* (2019) 'Multidisciplinary approaches for studying rhizobium–legume symbioses', *Canadian Journal of Microbiology*, 65(1), pp. 1–33. Available at: https://doi.org/10.1139/cjm-2018-0377.

diCenzo, G.C. and Finan, T.M. (2018) 'Techniques for large-scale bacterial genome manipulation and characterization of the mutants with respect to in silico metabolic reconstructions', in M. Fondi (ed.) *Metabolic Network Reconstruction and Modeling: Methods and Protocols*. New York, NY: Springer, pp. 291–314. Available at: https://doi.org/10.1007/978-1-4939-7528-0_13.

Engler, C. *et al.* (2009) 'Golden Gate Shuffling: A one-pot dna shuffling method based on Type IIs restriction enzymes', *PLoS ONE*, 4(5), p. e5553. Available at: https://doi.org/10.1371/journal.pone.0005553.

Engler, C. *et al.* (2014) 'A Golden Gate modular cloning toolbox for plants', *ACS Synthetic Biology*, 3(11), pp. 839–843. Available at: https://doi.org/10.1021/sb4001504.

Finan, T.M. *et al.* (1986) 'Second symbiotic megaplasmid in *Rhizobium meliloti* carrying exopolysaccharide and thiamine synthesis genes', *Journal of Bacteriology*, 167(1), pp. 66–72. Available at: https://doi.org/10.1128/jb.167.1.66-72.1986.

Gantner, J. *et al.* (2018) 'Peripheral infrastructure vectors and an extended set of plant parts for the Modular Cloning system', *PloS One*, 13(5), p. e0197185. Available at: https://doi.org/10.1371/journal.pone.0197185.

Geddes, B.A. *et al.* (2019) 'Engineering transkingdom signalling in plants to control gene expression in rhizosphere bacteria', *Nature communications*, 10(1), pp. 1–11. Available at: https://doi.org/10.1038/s41467-019-10882-x.

Geddes, B.A. *et al.* (2021) 'Minimal gene set from *Sinorhizobium* (*Ensifer*) *meliloti* pSymA required for efficient symbiosis with Medicago', *Proceedings of the National Academy of Sciences*, 118(2). Available at https://doi.org/10.1073/pnas.2018015118.

Geddes, B.A., Mendoza-Suárez, M.A. and Poole, P.S. (2019) 'A bacterial expression vector archive (BEVA) for flexible modular assembly of Golden Gate-compatible vectors', *Frontiers in Microbiology*, 9, p. 3345. Available at: https://doi.org/10.3389/fmicb.2018.03345.

Grützner, R. *et al.* (2021) 'High-efficiency genome editing in plants mediated by a Cas9 gene containing multiple introns', *Plant Communications*, 2(2), p. 100135. Available at: https://doi.org/10.1016/j.xplc.2020.100135.

Guerry, P., Van Embden, J. and Falkow, S. (1974) 'Molecular nature of two nonconjugative plasmids carrying drug resistance genes', *Journal of Bacteriology*, 117(2), pp. 619–630.

Hahn, F. *et al.* (2020) 'A modular cloning toolkit for genome editing in plants', *BMC plant biology*, 20(1), p. 179. Available at: https://doi.org/10.1186/s12870-020-02388-2.

Haskett, T.L. *et al.* (2022) 'Control of nitrogen fixation and ammonia excretion in *Azorhizobium Caulinodans*', *PLOS Genetics*, 18(6), p. e1010276. Available at: https://doi.org/10.1371/journal.pgen.1010276.

Haskett, T.L. *et al.* (2023) 'Rhizopine biosensors for plant-dependent control of bacterial gene expression', *Environmental Microbiology*, 25(2), pp. 383–396. Available at: https://doi.org/10.1111/1462-2920.16288.

Iverson, S.V. *et al.* (2016) 'CIDAR MoClo: Improved MoClo assembly standard and new *E. coli* part library enable rapid combinatorial design for synthetic and traditional biology', *ACS Synthetic Biology*, 5(1), pp. 99–103. Available at: https://doi.org/10.1021/acssynbio.5b00124.

Jorrin, B. *et al.* (2024) 'Stable, fluorescent markers for tracking synthetic communities and assembly dynamics', *Microbiome*, 12(1), p. 81. Available at: https://doi.org/10.1186/s40168-024-01792-2.

Kearsley, J.V., Sather, L.M. and Finan, T.M. (2024) '*Sinorhizobium* (*Ensifer*) *meliloti'*, *Trends in Microbiology*, 32(5):515-518. Available at: doi: 10.1016/j.tim.2024.03.004.

Kuhstoss, S. and Rao, R.N. (1991) 'Analysis of the integration function of the streptomycete bacteriophage φC31', *Journal of molecular biology*, 222(4), pp. 897–908.

Lee, H.H. *et al.* (2019) 'Functional genomics of the rapidly replicating bacterium Vibrio natriegens by CRISPRi', *Nature Microbiology*, 4(7), pp. 1105–1113. Available at: https://doi.org/10.1038/s41564-019-0423-8.

Lee, M.E. *et al.* (2015) 'A highly characterized yeast toolkit for modular, multipart assembly', *ACS Synthetic Biology*, 4(9), pp. 975–986. Available at: https://doi.org/10.1021/sb500366v.

Martínez-García, E. *et al.* (2023) 'SEVA 4.0: an update of the Standard European Vector Architecture database for advanced analysis and programming of bacterial phenotypes', *Nucleic Acids Research*, 51(D1), pp. D1558–D1567. Available at: https://doi.org/10.1093/nar/gkac1059.

Mendoza-Suárez, M.A. *et al.* (2020) 'Optimizing Rhizobium-legume symbioses by simultaneous measurement of rhizobial competitiveness and N2 fixation in nodules', *Proceedings of the National Academy of Sciences*, 117(18), pp. 9822–9831. Available at: https://doi.org/10.1073/pnas.1921225117.

Meyer, R., Figurski, D. and Helinski, D.R. (1975) 'Molecular vehicle properties of the broad host range plasmid RK2', *Science*, 190(4220), pp. 1226–1228.

Milunovic, B. *et al.* (2014) 'Cell growth inhibition upon deletion of four toxin-antitoxin loci from the megaplasmids of *Sinorhizobium meliloti*', *Journal of Bacteriology*, 196(4), pp. 811–824. Available at: https://doi.org/10.1128/JB.01104-13.

Moore, S.J. *et al.* (2016) 'EcoFlex: A multifunctional MoClo kit for *E. coli* synthetic biology', *ACS Synthetic Biology*, 5(10), pp. 1059–1069. Available at: https://doi.org/10.1021/acssynbio.6b00031.

Obst, U., Lu, T.K. and Sieber, V. (2017) 'A modular toolkit for generating *Pichia pastoris* secretion libraries', *ACS Synthetic Biology*, 6(6), pp. 1016–1025. Available at: https://doi.org/10.1021/acssynbio.6b00337.

Prentki, P. and Krisch, H.M. (1984) '*In vitro* insertional mutagenesis with a selectable DNA fragment', *Gene*, 29(3), pp. 303–313. Available at: https://doi.org/10.1016/0378-1119(84)90059-3.

Quandt, J. and Hynes, M.F. (1993) 'Versatile suicide vectors which allow direct selection for gene replacement in Gram-negative bacteria', *Gene*, 127(1), pp. 15–21. Available at: https://doi.org/10.1016/0378-1119(93)90611-6.

Rossi, M. *et al.* (1996) 'Characterization of the plasmid pMB1 from *Bifidobacterium longum* and its use for shuttle vector construction', *Research in microbiology*, 147(3), pp. 133–143.

Scholz, P. *et al.* (1989) 'Complete nucleotide sequence and gene organization of the broad-host-range plasmid RSF1010', *Gene*, 75(2), pp. 271–288.

Schweizer, H.P., Klassen, T. and Hoang, T. (1996) 'Improved methods for gene analysis and expression in *Pseudomonas'*. in T. Nakazawa, K. *et al.* (ed.) *Molecular Biology of Pseudomonads*. Washington, DC: American Society for Microbiology, pp. 229-237.

Silva-Rocha, R. *et al.* (2013) 'The Standard European Vector Architecture (SEVA): a coherent platform for the analysis and deployment of complex prokaryotic phenotypes', *Nucleic Acids Research*, 41(Database issue), pp. D666–D675. Available at: https://doi.org/10.1093/nar/gks1119.

Stuttmann, J. *et al.* (2021) 'Highly efficient multiplex editing: one-shot generation of 8× *Nicotiana benthamiana* and 12× Arabidopsis mutants', *The Plant Journal: For Cell and Molecular Biology*, 106(1), pp. 8–22. Available at: https://doi.org/10.1111/tpj.15197.

Thorpe, H.M. and Smith, M.C. (1998) '*In vitro* site-specific integration of bacteriophage DNA catalyzed by a recombinase of the resolvase/invertase family', *Proceedings of the National Academy of Sciences*, 95(10), pp. 5505–5510.

581 Wang, L. *et al.* (2021) ‘Highly efficient CRISPR-mediated base editing in *Sinorhizobium*
582 *meliloti*’, *Frontiers in Microbiology*, 12. Available at:
583 https://doi.org/10.3389/fmicb.2021.686008.

584 Williamson, R. W. *et al.* (in preparation) 'Evaluation of engineering potential in undomesticated
585 microbes with VECTOR'.
586
587 Weber, E. *et al.* (2011) ‘A modular cloning system for standardized assembly of multigene
588 constructs’, *PloS One*, 6(2), p. e16765. Available at:
589 https://doi.org/10.1371/journal.pone.0016765.

590 Werner, S. *et al.* (2012) ‘Fast track assembly of multigene constructs using Golden Gate cloning
591 and the MoClo system’, *Bioengineered Bugs*, 3(1), pp. 38–43. Available at:
592 https://doi.org/10.4161/bbug.3.1.18223.

593 Yenofsky, R.L., Fine, M. and Pellow, J.W. (1990) ‘A mutant neomycin phosphotransferase II
594 gene reduces the resistance of transformants to antibiotic selection pressure.’, *Proceedings of the*
595 *National Academy of Sciences of the United States of America*, 87(9), pp. 3435–3439. Available
596 at: doi: 10.1073/pnas.87.9.3435.

597